This article was downloaded by:
On: *14 January 2011*
Access details: *Access Details: Free Access*
Publisher *Taylor & Francis*
Informa Ltd Registered in England and Wales Registered Number: 1072954 Registered office: Mortimer House, 37-41 Mortimer Street, London W1T 3JH, UK

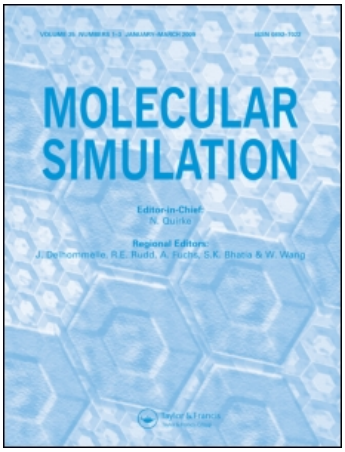

Molecular Simulation
Publication details, including instructions for authors and subscription information:
http://www.informaworld.com/smpp/title~content=t713644482

The influence of the simulation box geometry in solid-state molecular simulations: phase behaviour of lithium iodide in a dynamic Monte Carlo simulation

Björn Wittich[a]; Ulrich K. Deiters[a]
[a] Institute of Physical Chemistry, University of Cologne, Köln, Germany

Online publication date: 16 April 2010

To cite this Article Wittich, Björn and Deiters, Ulrich K.(2010) 'The influence of the simulation box geometry in solid-state molecular simulations: phase behaviour of lithium iodide in a dynamic Monte Carlo simulation', Molecular Simulation, 36: 5, 364 — 372
To link to this Article: DOI: 10.1080/08927020903483320
URL: http://dx.doi.org/10.1080/08927020903483320

PLEASE SCROLL DOWN FOR ARTICLE

Full terms and conditions of use: http://www.informaworld.com/terms-and-conditions-of-access.pdf

This article may be used for research, teaching and private study purposes. Any substantial or systematic reproduction, re-distribution, re-selling, loan or sub-licensing, systematic supply or distribution in any form to anyone is expressly forbidden.

The publisher does not give any warranty express or implied or make any representation that the contents will be complete or accurate or up to date. The accuracy of any instructions, formulae and drug doses should be independently verified with primary sources. The publisher shall not be liable for any loss, actions, claims, proceedings, demand or costs or damages whatsoever or howsoever caused arising directly or indirectly in connection with or arising out of the use of this material.

Molecular Simulation
Vol. 36, No. 5, April 2010, 364–372

Taylor & Francis
Taylor & Francis Group

The influence of the simulation box geometry in solid-state molecular simulations: phase behaviour of lithium iodide in a dynamic Monte Carlo simulation

Björn Wittich[1] and Ulrich K. Deiters*

Institute of Physical Chemistry, University of Cologne, Luxemburger Straße. 116, Köln 50321, Germany

(*Received 24 September 2009; final version received 12 November 2009*)

In thermodynamic computer simulations, it is common to use cubic simulation boxes, which are then regarded as unit cells of an infinitely large cubic lattice. While this approach is adequate for gases and liquids at low densities, for dense liquids and solid cuboid boxes forming an orthorhombic lattice or parallelepiped boxes forming a triclinic lattice are shown to be advantageous, because they do not predetermine the structure of the simulated system. In this work, an extension of the Ewald summation formalism towards a parallelepiped lattice symmetry is given. Monte Carlo simulations of lithium iodide with cubic, cuboid and parallelepiped box geometries are reported; the latter is found to offer little improvement over the cuboid geometry. The existence of two hexagonal solid phases is discussed.

Keywords: dynamic NPT; lithium iodide; box shape; phase behaviour

Downloaded At: 17:10 14 January 2011

1. Introduction

Lithium iodide is a salt with a rather small cation/anion size ratio of about 0.35. The ionic hard-spheres model therefore predicts a tetrahedral coordination of the lithium ions; consequently, lithium iodide should belong to the hexagonal space group (wurtzite lattice type). This, however, is in conflict with experiments: solid lithium iodide has a face-centred cubic (fcc) crystal structure. It is therefore not surprising that, since 1973, the lithium iodide system has been studied by several authors [1–4]. Experiments of Jansen et al. [5], in 2004, revealed the existence of a hexagonal phase at low temperatures and pressures.

About 40 years ago, Lewis et al. [1] performed computer simulations of alkali halides (including lithium iodide), using a cubic simulation box geometry. Although these simulations were a breakthrough in the simulation of ionic crystals, there were some problems with the thermodynamic properties of lithium iodide which the authors traced back to their interaction potential. They observed a 'spontaneous fusion' below the melting point.

This, however, might not have been the only reason for the problems: it is common to use cubic simulation boxes in thermodynamic computer simulations. Under the equally common assumption of periodic boundary conditions, these simulation boxes are thought to be surrounded by replicas. The resulting simulation ensemble is therefore a cubic lattice of infinite extension, of which the simulation box is the unit cell. It is conceivable that the cubic symmetry of the simulation box predetermines the structure of the simulated system. This should not be a problem for dilute isotropic systems (e.g. gases), but it might influence the outcome of simulations of solids of non-cubic symmetry similar to the one shown in the 1980s by Yashonath and Rao [6] on a Monte Carlo ensemble of caesium described by a simple Lennard-Jones potential. In contrast to Yashonath and Rao, we also include electric charges in our simulation, which is more difficult because of the long-range interactions and possibly resulting finite-size effects.

In this work, we report Monte Carlo simulations of liquid and solid lithium iodide, using the interaction potential of Lewis et al. [1] as well as a more recent one of Deppe et al. [3]. Furthermore, we compare simulations made with classical cubic simulation boxes and simulations made with parallelepiped boxes where lengths and angles fluctuate independently during the simulation. This requires a high accuracy in calculating the long-range forces to prevent artefacts.

2. Computer simulations

2.1 Simulation technique

The computer simulations were carried out with a standard Metropolis Monte Carlo technique, using an NPT ensemble. The ensemble size was usually 256 LiI ion pairs. The simulations involved typically 10^4 cycles, with a cycle consisting of (attempted) random displacements of all ions, followed by three (attempted) volume changes. In contrast to the conventional Monte Carlo technique, however, the lengths, widths, depths and angles of the simulation box were allowed to fluctuate independently.

*Corresponding author. Email: ulrich.deiters@uni-koeln.de

ISSN 0892-7022 print/ISSN 1029-0435 online
© 2010 Taylor & Francis
DOI: 10.1080/08927020903483320
http://www.informaworld.com

Downloaded At: 17:10 14 January 2011

Unless stated otherwise, periodic boundary conditions were assumed; the minimum image convention was applied to the calculation of interaction energies between particles.

Standard Metropolis rules [7] were used to decide the acceptance or rejection of trial moves. In detail, this means that the acceptance probability for particle movements was

$$p_{\mathrm{pm}}(\mathrm{o} \rightarrow \mathrm{n}) = \begin{cases} 1 & \text{if } \Delta U_{\mathrm{o}\rightarrow\mathrm{n}} < 0, \\ \exp(-\beta(\Delta U_{\mathrm{o}\rightarrow\mathrm{n}})) & \text{otherwise,} \end{cases} \quad (1)$$

where $\Delta U_{\mathrm{o}\rightarrow\mathrm{n}}$ denotes the difference in the internal energies of the new and the old configurations.

The acceptance rules for changes in the simulation box size and shape were also based on the Metropolis acceptance scheme. After a particle movement, a randomly chosen side of the box was stretched with a probability of $3/(N+3)$ by a randomly determined factor. The coordinates of the atoms were also scaled with this factor. The probability $p_{\mathrm{vc}}(\mathrm{o} \rightarrow \mathrm{n})$ of acceptance was proportional to

$$p_{\mathrm{vc}}(\mathrm{o} \rightarrow \mathrm{n}) = \begin{cases} 1, & \text{if } a > 1, \\ a, & \text{otherwise,} \end{cases} \quad (2)$$

with $a = \exp(-\beta[\Delta U + p\Delta V - (N+1)\beta^{-1}\ln(V_{\mathrm{n}}/V_{\mathrm{o}})])$. Here, N is the number of particles, β is $1/k_{\mathrm{B}}T$, 'o' means the old and 'n' the new configurations. The trial moves – displacements and box deformations – were calculated from uniform probability distributions. The extents of these distributions, maximal displacements and deformation parameters were adjusted to give an average acceptance ratio of 0.30.

2.2 Interaction potentials

The most common type of interaction potential used for simple single-ionic systems is the Born–Huggins–Mayer–Fumi–Tosi potential [8–10] used by Lewis et al. [1],

$$\phi_{i,j}(r) = \frac{1}{4\pi\epsilon_0}\frac{q_i q_j}{r_{i,j}} + b\exp(B(\sigma_{i,j} - r)) + C_{i,j}r^{-6} + D_{i,j}r^{-8}. \quad (3)$$

The first term represents the Coulomb interaction between ions i and j, the second one represents the electronic repulsion at short distances and the remaining ones represent the dipole–dipole and the dipole–quadrupole dispersion effects. The minimum image convention was applied to the calculation of the last three terms of Equation (3). The potential cut-off distance for these terms was ≥ 9 Å. The contribution of the Coulomb term, whose slow ($\propto r^{-1}$) decrease with distance would cause an unacceptable error, was calculated by means of the Ewald sum. A detailed formulation of the Ewald sum for the cuboid and parallelepiped box geometry is given in the appendix. The parameters for this interaction potential are given in Table 1.

More recently, Deppe et al. [3] proposed another interaction potential for lithium iodide,

$$\phi_{i,j}(r) = \frac{1}{4\pi\epsilon_0}\frac{q_i q_j}{r_{i,j}} + \frac{b}{r_{i,j}^4}\exp(-k(r_{i,j} - \sigma_{i,j})) + C_{i,j}r_{i,j}^{-6} + D_{i,j}r_{i,j}^{-8} + E_{i,j}r_{i,j}^{-9}. \quad (4)$$

The parameters of this potential are given in Table 2. It differs from the previous potential by the distance dependence of the electronic repulsion term and an additional r^{-9} term. The two interaction potentials are compared in Figure 1.

It should be noted that both potential functions have physically meaningless attraction wells at small distances. It is therefore necessary to exclude distances below a threshold r_{excl}, i.e. to assume hard cores inside the ions.

2.3 Common-neighbour analysis

The common-neighbour analysis (CNA) is a method for analysing the geometric environment of the nearest neighbours around a reference atom n, as shown in Figure 2. In the first step, the CNA cut-off for the first coordination shell is determined from the first minimum of the monoatomic radial distribution function (RDF). All atoms at larger distances are neglected. For each atom m within this CNA cut-off distance, the following geometric analysis is performed:

(1) The common neighbours, i.e. all atoms that are in the common CNA cut-off of both m and n, are counted $\rightarrow i$.
(2) A geometric bond is constructed between those of the i common neighbours that are less than the CNA cut-off distance apart; these bonds are counted $\rightarrow j$.

Table 1. Parameters of lithium iodide of [1] used for Equation (3).

	Interaction		
Parameter	++	+ −	− −
σ (10^{-10} m)	1.632	2.723	3.814
C (10^{-79} J m^6)	−0.073	−3.3	−378.0
D (10^{-99} J m^8)	−0.03	−5.3	−1060.0
r_{excl} (10^{-10} m)	0.5	1.15	1.8
B (10^{-10} m^{-1})	2.33	2.33	2.33
b (10^{-19} J)	0.67600	0.46475	0.25350

Table 2. Parameters of lithium iodide of [3] used for Equation (4).

	Interaction		
Parameter	++	+ −	− −
σ (10^{-10} m)	0.95	3.00	2.05
C (10^{-79} J m^6)	−8.54	−25.0	−266.0
D (10^{-99} J m^8)	−36.8	−114.0	−1000.0
E (10^{-109} J m^9)	−10.0	−6.5	−400.0
r_{excl} (10^{-10} m)	1.2	1.7	2.2
k (10^{10} m^{-1})	1.1	1.1	1.1
b (10^{-58} J m^4)	2.8	2.8	2.8

(3) The number of bonds of the longest chain that can be formed among these j bonds is determined $\rightarrow k$.

i, j and k are then reported together with the number of neighbours of n having this set of counts.

For example, the fcc structure has the signature 12×421 (12 equivalent nearest neighbours for each atom); the hexagonal close-packing (hcp) structure has the signature $6 \times 421 + 6 \times 422$ (two sets of six nearest neighbours with slightly different environments). A detailed explanation of the CNA has been given by Lümmen and Kraska [11].

Lümmen and Kraska [11] developed a new CNA algorithm for analysing binary structures. This method is very efficient for binary systems with atoms of a size ratio of 0.9–1.0. But as the hard-core diameters of Li^+ and I^- differ very much, we preferred using a conventional algorithm and analysing the first coordination sphere of counterions only. The CNA cut-off of this coordination sphere is determined by the first minimum of the monoatomic RDF.

3. Results

3.1 Bulk-phase (NPT) simulations with the potential of Lewis et al.

For static simulations of bulk phases of lithium iodide with the potential of Lewis et al. [1], we found that the cubic

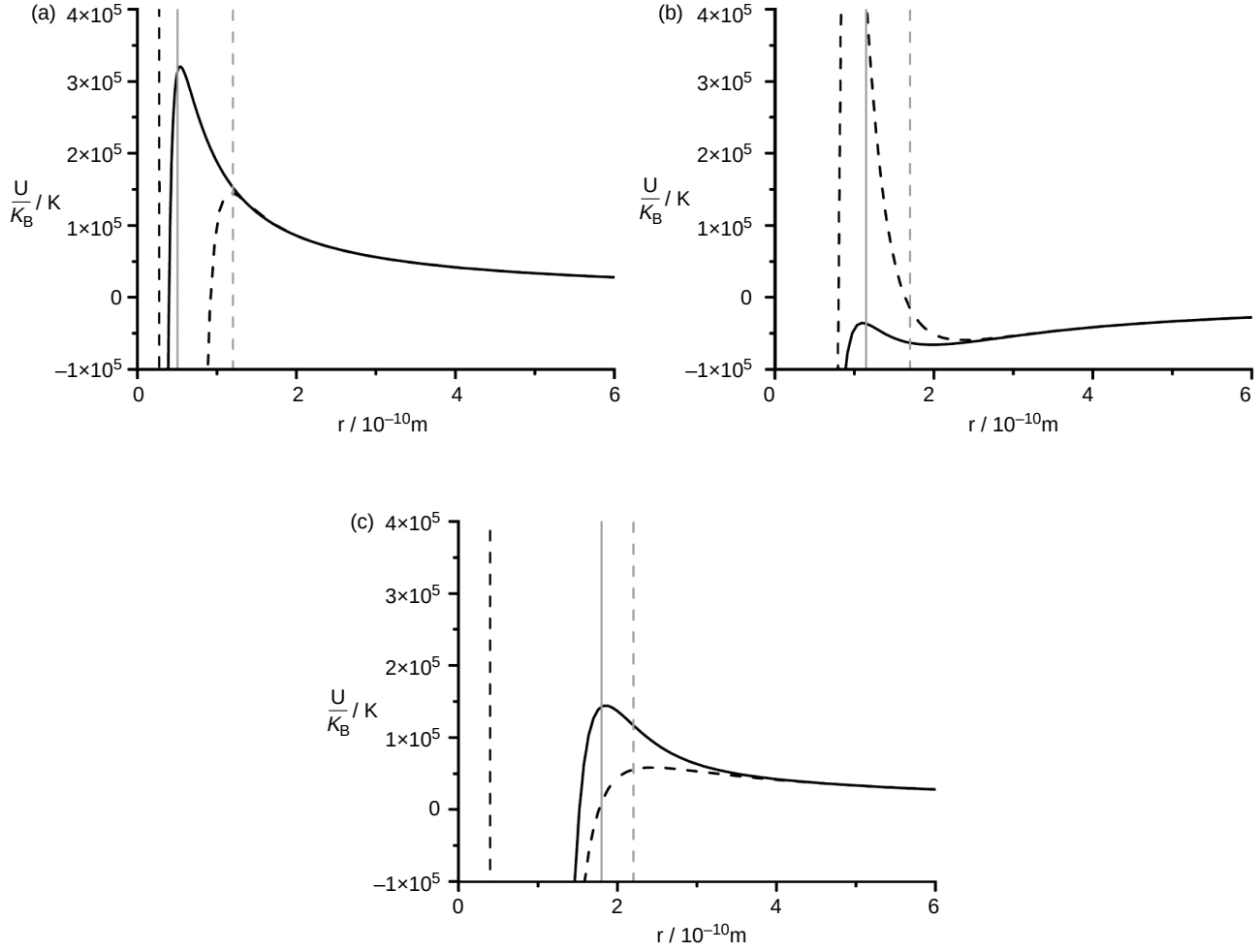

Figure 1. Comparison of pair potentials. - - -, Deppe et al. [3], Equation (4); – –, Lewis et al. [1], Equation (3); the light grey lines indicate the hard-core cut-off. (a) Cation–cation, (b) cation–anion and (c) anion–anion potential.

Downloaded At: 17:10 14 January 2011

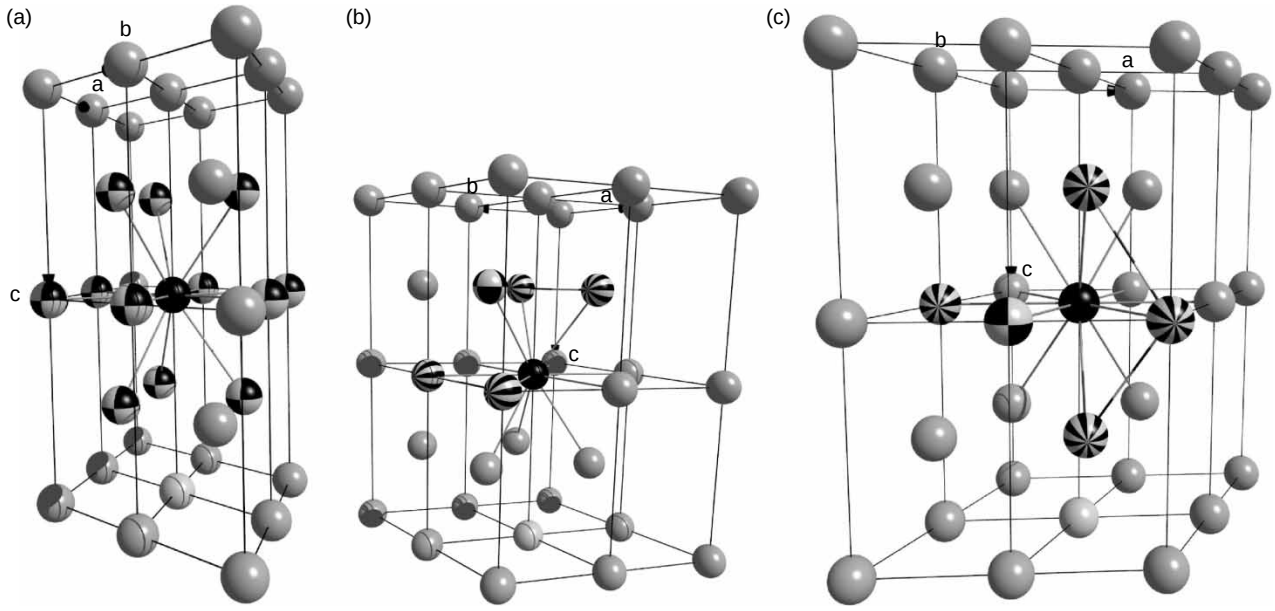

Figure 2. Monoatomic CNA method: (a) the reference atom n is located in the middle of the $2 \times 2 \times 2$ supercell and coloured in black. The 12 checked atoms represent all the atoms lying within the CNA cut-off. (b) The four striped atoms are lying within the CNA cut-off distance of the reference atom (black) and that of one of the 12 checked atoms m. Two pairs of the striped atoms have a distance smaller than the CNA cut-off, so that two bonds can be created, hence $j = 2$. The longest chain has the length $k = 1$. The resulting signature is 421. (c) The four striped atoms are lying within the CNA cut-off distance of the reference atom (black) and that of one of the 12 checked atoms m, which are now situated in the *ab* plane of the reference atom. Three of the striped atoms have a distance smaller than the CNA cut-off, so that two bonds can be created ($j = 2$); now the longest uninterrupted chain has the length $k = 2$.

Downloaded At: 17:10 14 January 2011

crystal structure (the initial configuration for all such simulations) transformed into the wurtzite structure when the restriction to a cubic box symmetry was given up. This becomes evident from a comparison of the RDFs obtained for a cubic or a cuboid simulation box with the ideal functions for an fcc or a wurtzite structure, as shown in Figure 3. This result is also supported by CNA [12].

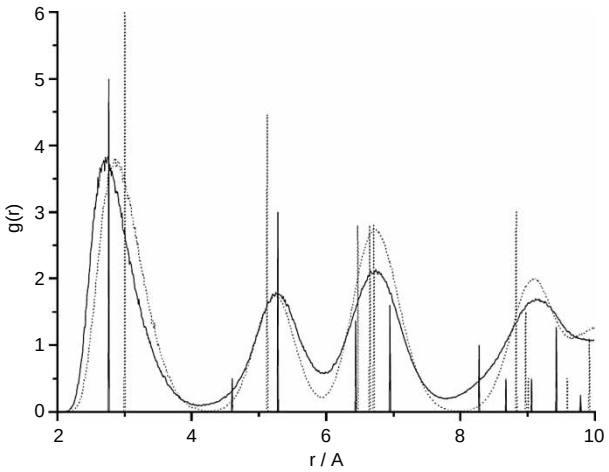

Figure 3. Cation–anion RDFs obtained with different simulation box geometries with the pair potential of Lewis et al. [1]. —, cuboid; . . . , cubic. The sharp peaks represent functions of the ideal structures at zero temperature: —, wurtzite; . . . , fcc.

3.1.1 Cubic box

For a CNA cut-off of $r_{\min}$ of 5.18 Å in the monoatomic CNA, we found that all 256 Li and I particles had the ideal fcc signature. In the binary analysis, we chose a CNA cut-off of $r_{\min} = 4.0$ Å. All 512 particles were octahedrally coordinated, but with distorted angles. The octahedral configurations of the Li and I atoms do not evidently correspond to energy minima. This is a clear example where the shape of the cubic box prevents the lattice to transform into another structure. Lewis et al. had observed this phenomenon, but attributed it to too large polarisability parameters. They had also noticed that the RDF in their simulation differed from the RDFs of other fcc ion crystals such as NaCl or KCl.

3.1.2 Parallelepiped and cuboid boxes

In simulations with a parallelepiped simulation box, we observed that, after starting from a cubic box, the box dimensions changed immediately, whereas its angles remained constant at about 90°. Repeating the simulation with fixed square angles (cuboid box) resulted in the same structural and thermodynamic properties. For a CNA cut-off $r_{\min}$ of 5.40 Å, we found that 147 out of the 256 ions had an ideal hcp signature; 26 ions still had the signature of the initial configuration (fcc). In the binary case, with a CNA cut-off of 3.4 Å, we found that 510 out of the 512 ions were tetrahedrally coordinated.

Because these results do not agree with the experimental data, we discarded the potential of Lewis et al. [1] and used the potential of Deppe et al. [3] for all the following simulations.

3.2 Bulk-phase (NPT) simulations with the potential of Deppe et al.

Repeating these simulations with the pair potential of Deppe et al. [3], we found that this potential is able to describe the correct structures of lithium iodide at normal conditions. Giving up the restriction of the cubic box does not lead to a different structure as with the previous potential. With this potential, the fcc structure is the most stable one. All particles have the expected signatures. The parameters of the structure, which are in excellent agreement with experiments, are given in Table 3.

3.3 Epitaxial resublimation of lithium iodide gas onto an oriented sapphire substrate

This simulation was meant to reproduce an experiment of Jansen et al. [5], by which the hexagonal phase of LiI had been obtained by resublimation of LiI vapour onto the (001) surface of a sapphire substrate.

Five hundred LiI particles were randomly placed into a large simulation box at 1000 K to represent the vapour phase. In the centre of the box, a small fixed crystal (500 ions) of corundum (Al_2O_3) structure was placed; the electric charge of the Al ions was set to +3, the charge of the oxygen to −2. The geometry of this seed crystal was fixed during the simulation [13]. As in the experiment, the crystal was maintained at 73 K. Particles from the vapour phase coming within a cut-off distance of 3 Å of the (001) crystal surface were cooled down to 73 K; particles detaching from the crystal surface were heated up to 1000 K when their distance exceeded 3 Å, and were no longer considered parts of the solid phase.

We found that the resublimated particles formed a wurtzite-like phase (Figure 4(a)), in which all ions were tetrahedrally coordinated. The first maximum of the Li–I RDF of the epitaxial LiI layer was exactly the same as the experimental value [5]. The first peaks of the Li–Li and I–I RDFs were slightly shifted to smaller distances. This is probably due to the relatively small size of the simulation ensemble. Because of the long range of the electrostatic potential, the ions in the 'sapphire' substrate deformed the tetrahedral units of the LiI crystal to trigonal pyramids, but the cation–anion distance was maintained. The deformation decreased when the crystal became larger. The simulated crystallographic data are given in Table 3; they are in excellent agreement with experiments.

3.4 A new hexagonal phase of LiI

Starting from a hexagonal (wurtzite-like) LiI crystal, we performed NPT Monte Carlo simulations at 300 K and 0.1 MPa. If periodic boundary conditions were observed, i.e. a crystal of infinite size was simulated, the structure spontaneously changed to $P6_3/mmc$ symmetry (the space group of hexagonal boron nitride, h-BN), as shown in Figure 5. A further transition to the stable fcc structure was kinetically inhibited. Only at pressures of about 1 GPa, the activation energy became low enough to permit the spontaneous transition to the fcc structure.

In an NVT simulation without periodic boundary conditions, i.e. for a finite-size crystal having surfaces, a LiI crystal of h-BN structure was found to change to the fcc structure at 300 K and 0.1 MPa spontaneously. An example of the resulting domains is shown in Figure 6. This transformation was checked for different sizes of the crystal (256, 512 and 1024 particles).

When the periodic boundary condition was only applied to the (x, y) plane, i.e. for a two-dimensional layer of LiI, the transition to the fcc phase was hindered.

3.4.1 Phase transition from wurtzite to $P6_3/mmc$

The best way to understand the mechanism is looking at a small region of the bulk structure (Figure 5(c)). In this figure, it is easy to recognise that the blue LiI_4 and the red Li_4I tetrahedra have parallel-oriented sides which are situated in the (x, y) plane. During the phase transformation, the central atoms of the tetrahedra move downwards

Table 3. Crystallographic data at 1 K, 0 MPa.

	β-LiI	α-LiI	New phase
Symmetry	Hexagonal	Cubic	Hexagonal
Space group, Z	$P6_3mc$ (no. 186), 2	$Fm\bar{3}m$ (no. 225), 4	$P6_3/mmc$ (no. 194), 2
Cell parameters (pm)	$a = 451$[a]	$a = 584$[b]	$a = 490$[b]
	$c = 731$		$c = 579$
Cell volume (10^6 pm^3)	129.0	199.2	120.4
Molar volume (cm^3 mol^{-1})	38.9	29.95 ± 0.01	34.03 ± 0.01
Lattice energy (kJ mol^{-1})	−707.49	−722.04	−714.60
Lattice energy (300 K)/kJ mol^{-1}	Unstable	−714.16 ± 0.28	−706.70 ± 0.30

Notes: [a]Calculated from Section 3.3. [b]Calculated from bulk simulation.

Downloaded At: 17:10 14 January 2011

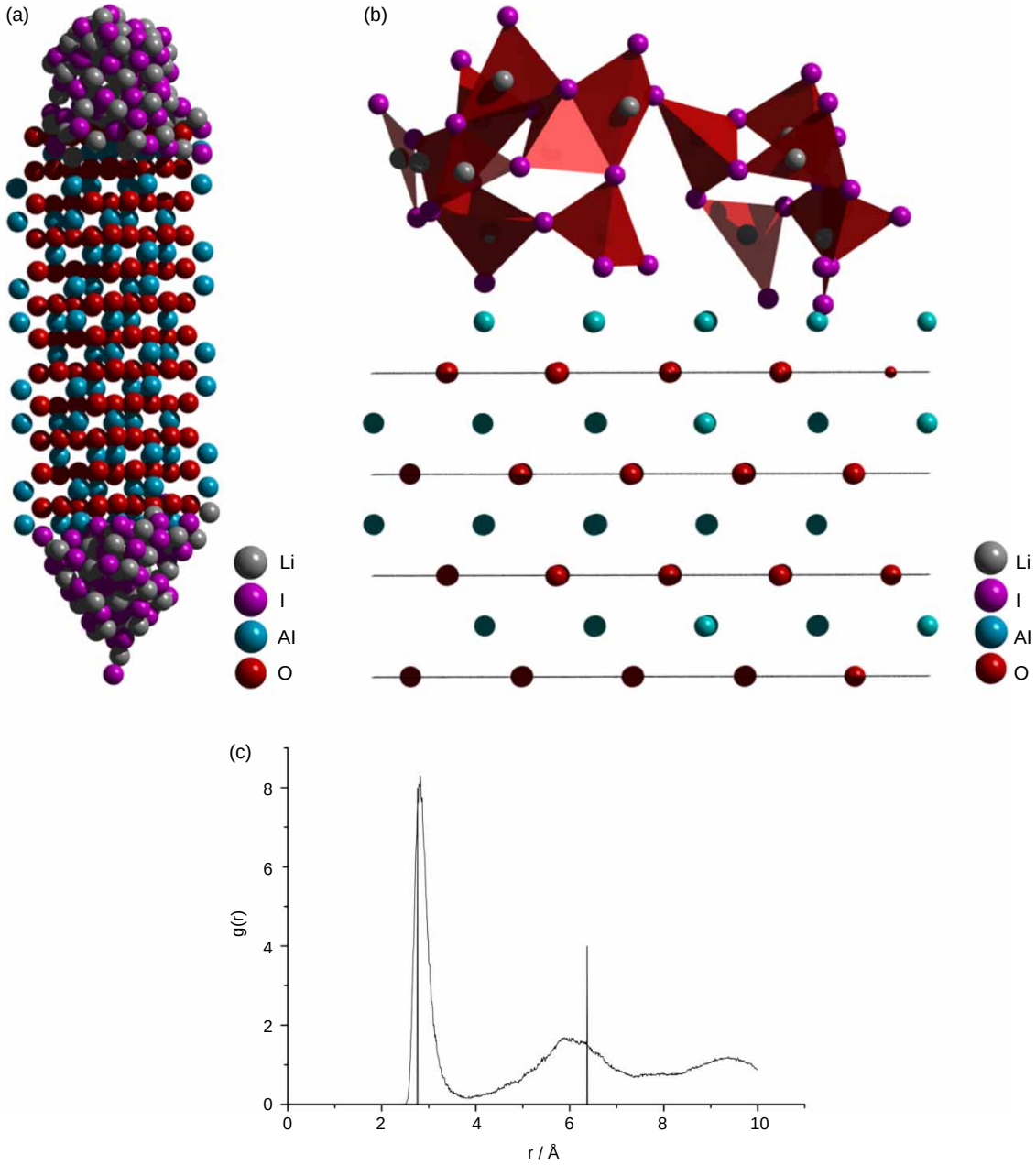

Figure 4. Resublimation of gaseous lithium iodide onto a cooled fixed crystal of corundum: (a) sapphire crystal with resublimated LiI on the 001 surfaces. (b) Cross-section of a 001 surface; the tetrahedra show the tetrahedral configuration of the Li–I domains. (c) Li–I RDF; the sharp peaks indicate the ideal configuration.

along the *c*-axis, so that they come to lie between the counterions in the (*x*, *y*) plane. Almost all ion movements are in the direction of the *c*-axis. The transition can also be explained with the help of Figure 5(a),(b): decreasing two 109° angles of the wurtzite structure to 90° leads to the $P6_3/mmc$ structure with a slightly decreased cell size *c*.

3.4.2 *Phase transition from $P6_3/mmc$ to fcc*

At ambient pressure, the activation energy for the transition to the most stable structure with six-fold-coordinated central atoms is too large in the infinite crystal. Therefore, the transition can occur at high pressure or in small crystals only.

The atom movements associated with this transition take place in the (*x*, *y*) plane. From Figure 7(a), which shows a projection of the crystal structure along the *c*-axis, one can see that two of the 120° angles shrink to 90°; the resulting vacancy is taken up by a counterion from the neighbourhood, which leads to the simple fcc structure (Figure 7(c)). An overview of the energies of the LiI structures is given in Figure 8.

Downloaded At: 17:10 14 January 2011

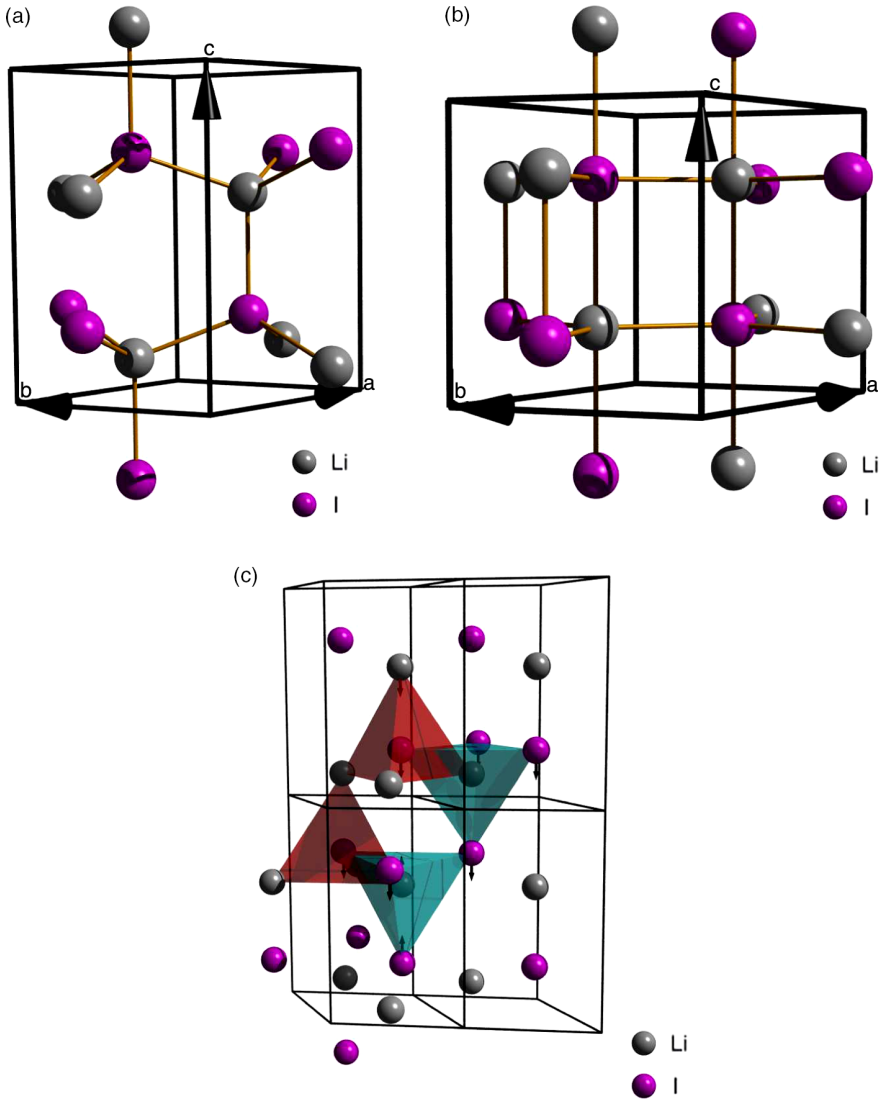

Figure 5. Structure of wurtzite and $P6_3/mmc$: (a) elementary cell of wurtzite, (b) elementary cell of $P6_3/mmc$ and (c) mechanism of phase transition.

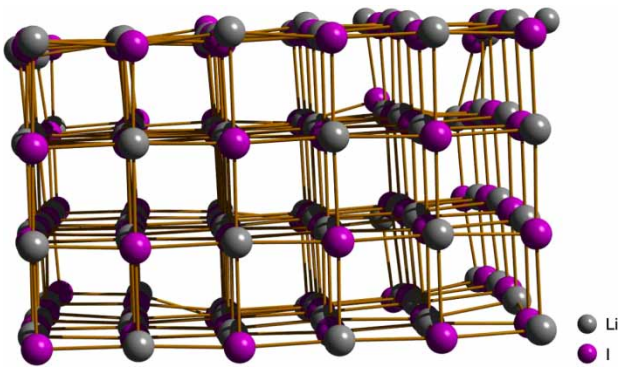

Figure 6. Resulting domains of the fcc structure (the start configuration was the h-BN structure of LiI) at 300 K for a finite crystal (NVT).

4. Conclusion

In this work, we demonstrate the importance of a variable box geometry in computer simulations of dense phases, especially of solids and high-density fluid phases. The largest improvements in convergence behaviour are obtained by letting the simulation box relax from a cubic to a cuboid shape. The next step, the relaxation to a parallelepiped box, gave no significant improvement for the LiI system; the box angles remained near 90°. This is not surprising, for changing the box angles during a simulation usually leads to distorted configurations with a high probability of particle overlapping. Nevertheless, in simulations of dense bulk structures, this most general kind of box geometry should be preferred in order to avoid any bias.

Downloaded At: 17:10 14 January 2011

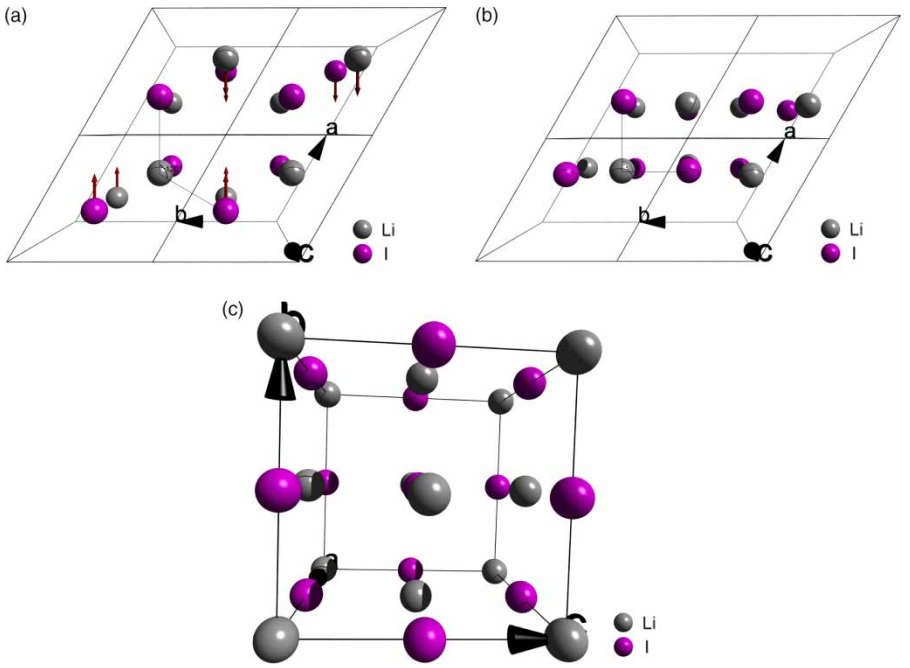

Figure 7. Structures of hexagonal $P6_3/mmc$ and cubic LiI: (a) 2×2 elementary cells of $P6_3/mmc$, (b) resulting fcc structure (in a hexagonal cell) and (c) resulting fcc structure (in a cubic cell).

Downloaded At: 17:10 14 January 2011

Of course, the bias introduced by a cubic simulation box geometry can also be reduced simply by using a larger box and, consequently, more particles. But this leads to another problem: the mechanisms of the phase transitions involve concerted movements of many particles, and the larger the particle number is chosen, the less likely such concerted movements become. As a consequence, the CPU time required for the simulation of a phase transition, which usually scales with $N^{1.5}$–N^2, or with $N \log N$ for the particle mesh algorithm, now increases with a higher power of the particle number. We observed this in the simulation 3.1, where an ensemble of 256 particles needed considerably less time for the phase transition than that of 512 particles, but still gave the same molar configurational energy as the larger ensemble.

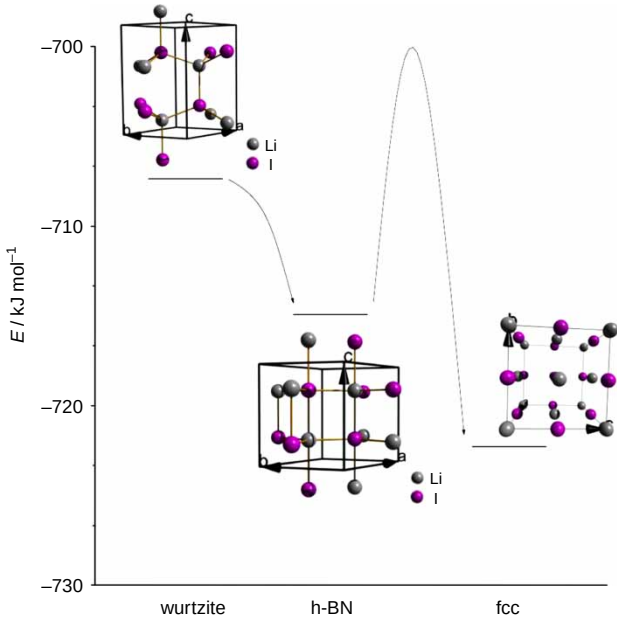

Figure 8. Energy landscape of LiI structures observed in this work, together with indications of activation energies.

The pair potential of Lewis et al. [1] leads to wrong predictions for the phase behaviour of lithium iodide, whereas the potential of Deppe et al. [3] is able to generate the thermodynamically stable fcc structure and the metastable wurtzite structure. The crystallographic and thermodynamic properties of the phases agree well with the experimental data.

Furthermore, the simulations indicate the existence of a new phase with the structure $P6_3/mmc$ (h-BN), which has not been found experimentally, yet. The lattice energy of the new phase is between those of the fcc and the wurtzite structure (cf. 3). The transition from the new structure to the stable fcc structure is kinetically hindered at low pressures. The mechanisms of the transitions between the hcp, h-BN and fcc structure of LiI immediately lead to a possible experimental route to h-BN LiI: it would be necessary to start from an hcp (wurtzite-like) LiI crystal which is as large as possible in the *c* direction, because the hcp → h-BN transition requires ion displacements along this crystal axis. If the crystal is large enough in the *a* and *b* directions, the transition h-BN → fcc is kinetically inhibited, so that it should be possible to isolate the h-BN lithium iodide.

Note

1. Email: bjoern.wittich@uni-koeln.de

References

[1] J.W.E. Lewis, K. Singer, and L.V. Woodcock, *Thermodynamic and structural properties of liquid ionic salts obtained by Monte Carlo computation*, J. Chem. Soc. Faraday Trans. II 71 (1975), pp. 301–312.

[2] J. Michielsen, P. Woerlee, F.V. Graaf, and J.A.A. Ketelaar, *Pair potential for alkali metal halides with rock salt crystal structure*, Faraday Trans. 71 (1975), pp. 1730–1741.

[3] J. Deppe, M. Balkanski, R.F. Wallis, and A.R. McGurn, *Molecular-dynamics study of the lattice-vibration contribution to the frequency-dependent dielectric constant of lithium iodide*, Phys. Rev. B 45 (1992), pp. 5687–5690.

[4] Ž.P. Čančarević, J.C. Schön, D. Fischer, and M. Jansen, *Theoretical and experimental exploration of the energy landscape of LiI*, Mater. Sci. Forum 494 (2005), pp. 61–66.

[5] D. Fischer, A. Müller, and M. Jansen, *Existiert eine Wurtzit-Modifikation von Lithiumbromid? – Untersuchungen im System LiBr/LiI*, Z. Anorg. Allg. Chem. 630 (2004), pp. 2697–2700.

[6] S. Yashonath and C.N.R. Rao, *A Monte Carlo study of crystal structure transformations*, Mol. Phys. 54 (1985), pp. 245–251.

[7] D. Frenkel and B. Smit, *Understanding Molecular Simulation*, 2nd ed., Academic Press, San Diego, CA, 2002.

[8] M. Born and J.E. Mayer, *Zur Gittertheorie der Ionenkristalle*, Z. Phys. 75 (1932), pp. 1–18.

[9] M.L. Huggins and J.E. Mayer, *Interatomic distances in crystals of the alkali halides*, J. Chem. Phys. 1 (1933), pp. 643–646.

[10] M.P. Tosi and F.C. Fumi, *Ionic sizes and Born repulsive parameters in the NaCl-type alkali halides. I. Huggins–Mayer and Pauling forms*, J. Phys. Chem. Solids 25 (1964), pp. 31–43.

[11] N. Lümmen and T. Kraska, *Common neighbour analysis for binary atomic systems*, Model. Simul. Mater. Sci. Eng. 15 (2007), pp. 319–334.

[12] J.D. Honeycutt and H.C. Andersen, *Molecular dynamics study of melting and freezing of small Lennard-Jones clusters*, J. Phys. Chem. 91 (1987), pp. 4950–4963.

[13] J. Lewis, D. Schwarzenbach, and H.D. Flack, *Electric field gradients and charge density in corundum, α-Al_2O_3*, Acta Cryst. A38 (1982), pp. 733–739.

[14] M.P. Allen and D.J. Tildesley, *Computer Simulation of Liquids*, 1st ed., Oxford Science Publications, Oxford, 1988.

[15] D. Fincham, *Optimization of the Ewald sum for large systems*, Mol. Simul. 13 (1994), pp. 1–9.

Downloaded At: 17:10 14 January 2011

Appendix. The Ewald sum

The Ewald sum as a technique for the summation of diverging electrostatic energy terms has been explained in many textbooks [7,14]; there is no need to give a derivation here. We observe, however, that it has been given incorrectly in many places, sometimes even with mismatching units; furthermore, it is usually given for cubic simulation boxes only.

The Coulomb potential of the whole ionic system is

$$U = U_{\text{real}} + U_{\text{recip}}. \tag{A1}$$

The real-space part for the non-cubic box with the lengths L_x, L_y and L_z is

$$U_{\text{real}} = \frac{1}{4\pi\epsilon_0}\frac{1}{2}\sum_i^N\sum_j^N q_i q_j \sum_{n_x=-\infty}^{\infty}\sum_{n_y=-\infty}^{\infty}\sum_{n_z=-\infty}^{\infty}{}' \frac{\operatorname{erfc}(\alpha|\vec{r}_{ij}+\vec{L}_n|)}{|\vec{r}_{ij}+\vec{L}_n|}, \tag{A2}$$

where N is the number of atoms; q_i, the charge of particle i; α, the Ewald shape parameter of the Gaussian function; $\vec{r}_{ij}$, the distance vector between particles i and j; and $\vec{L}_n = (n_xL_x, n_yL_y, n_zL_z)$. The prime indicates that all combinations with $j = i$ and $n_x = n_y = n_z = 0$ are omitted.

The reciprocal-space portion that is summed over all reciprocal vectors $\vec{k}$ is defined by:

$$U_{\text{recip}} = \frac{1}{4\pi\epsilon_0}\sum_{n_x=-\infty}^{\infty}\sum_{n_y=-\infty}^{\infty}\sum_{\vec{n}_z=-\infty}^{\infty}{}' \frac{2\pi}{k_n^2 V}\exp\left(\frac{-k_n^2}{4\alpha^2}\right) \times\left[\left(\sum_i^N q_i\cos(\vec{k}_n\cdot\vec{r}_i)\right)^2+\left(\sum_i^N q_i\sin(\vec{k}_n\cdot\vec{r}_i)\right)^2\right] - U_{\text{self}}. \tag{A3}$$

The prime indicates that the zero vector is forbidden. The reciprocal vectors are

$$\vec{k}_n = 2\pi(\mathbf{D}^T)^{-1}\vec{n}, \tag{A4}$$

and the matrix $\mathbf{D}$ is defined as

$$\mathbf{D} = \begin{pmatrix} a_{1x} & a_{2x} & a_{3x} \\ a_{1y} & a_{2y} & a_{3y} \\ a_{1z} & a_{z2} & a_{3z} \end{pmatrix}. \tag{A5}$$

Its elements are the components of the three cell vectors. The integer vector is given by

$$n = \begin{pmatrix} n_x \\ n_y \\ n_z \end{pmatrix}. \tag{A6}$$

The self-interaction, which must be subtracted, is given by

$$U_{\text{self}} = \frac{1}{4\pi\epsilon_0}\sum_i^N q_i^2\frac{\alpha}{\sqrt{\pi}}. \tag{A7}$$

The infinite sums of Equation (A2) are truncated at $|\vec{r}_{ij}+\vec{L}_n| = |\vec{r}_{\text{cut-off}}|$, and those of Equation (A4) at $|\vec{k}_n| = |\vec{k}_{n,\max}|$.

The parameters of the Ewald summation method used here are

$$|r_{\text{cut-off}}| = \frac{1}{2}|L_{\text{short}}|, \tag{A8}$$

$$\alpha = \frac{\pi}{|r_{\text{cut-off}}|} = \frac{2\pi}{|L_{\text{short}}|}, \tag{A9}$$

$$|k_{n,\max}| = \frac{4\pi^2}{|L_{\text{short}}|} = 2\pi\alpha, \tag{A10}$$

with the real-space cut-off $|r_{\text{cut-off}}|$ and the reciprocal cut-off $|k_{n,\max}|$; L_{short} is the length of the shortest box edge. This choice of parameters is considered optimal for middle-sized systems (about 500–1000 spherical particles) and the algorithm used in this work [15].

As α and the reciprocal cut-off are inversely proportional to L_{short}, any departure from the cubic shape of the simulation box results in an increase in the CPU time.

In order to check the validity of the above equations as well as our computer code, the energy of a static crystal composed of $2\times4\times8$ elementary cells was compared with that of a $4\times4\times4$ arrangement. It turned out that the differences in the ionic energies were negligible and even smaller than the cut-off errors of the repulsion and dispersion parts of the interaction potential.